IL-18 serum concentration is markedly elevated in typical familial Mediterranean fever with M694I mutation and can distinguish it from atypical type.	Yamazaki T, Shigemura T, Kobayashi N, Honda K, Yazaki M, Masumoto J, Migita K, Agematsu K	Mod Rheumatol. 2014 Dec 22:1-3.	2014	国外
Clinical course in a patient with neutrophil-specific granule deficiency and rapid detection of neutrophil granules as a screening test.	Shigemura T, Yamazaki T, Shiohara M, Kobayashi N, Naganuma K, Koike K, Agematsu K	J Clin Immunol. 2014 Oct;34(7):780-3	2014	国外
Markedly elevated CD64 expressions on neutrophils and monocytes are useful for diagnosis of periodic fever, aphthous stomatitis, pharyngitis, and cervical adenitis (PFAPA) syndrome during flares.	Yamazaki T, Hokibara S, Shigemura T, Kobayashi N, Honda K, Umeda Y, Agematsu K	Clin Rheumatol. 2014 May;33(5):677-83	2014	国外
Peripheral blood flow monitoring in an infant with septic shock.	Ishiguro A, Sakazaki S, Itakura R, Fujinuma S, Oka S, Motojima Y,Sobajima H, Tamura M	Pediatr Int. 2014 Oct;56(5):787-9.	2014	国外
Skin blood flow as a predictor of intraventricular hemorrhage in very-low-birth-weight infants.	Ishiguro A, Suzuki K, Sekine T, Sudo Y, Kawasaki H, Itoh K, Kanai M, Kato I, Sobajima H, Tamura M	Pediatr Res.	2014	国外
Intraperitoneal and intravenous deliveries are not comparable in terms of drug efficacy and cell distribution in neonatal mice with hypoxia-ischemia.	Ohshima M, Taguchi A, Tsuda H, Sato Y, Yamahara K, Harada-Shiba M, Miyazato M, Ikeda T, Iida H, Tsuji M.	Brain & Development	in press	国外
Administration of umbilical cord blood cells transiently decreased hypoxic–ischemic brain injury in neonatal rats	Hattori, T. Sato, Y. Kondo, T. Ichinohashi, Y. Sugiyama, Y. Yamamoto, M. Kotani, T. Hirata, H. Hirakawa, A. Suzuki, S. Tsuji, M. Ikeda, T. Nakanishi, K. Kojima, S. Blomgren, K. Hayakawa, M.	Dev Neurosci	Published online: February 17, 2015	国外

（注１）発表者氏名は、連名による発表の場合には、筆頭者を先頭にして全員を記載すること。

（注２）本様式はexcel形式にて作成し、甲が求める場合は別途電子データを納入すること。

SpringerPlus
a SpringerOpen Journal

RESEARCH Open Access

Glucocorticoids promote neural progenitor cell proliferation derived from human induced pluripotent stem cells

Eiichi Ninomiya[1], Taeka Hattori[1], Masashi Toyoda[2], Akihiro Umezawa[3], Takashi Hamazaki[1] and Haruo Shintaku[1*]

Abstract

Glucocorticoids (GCs) are frequently used for treating and preventing chronic lung disease and circulatory dysfunction in premature infants. However, there is growing concern about the detrimental effects of systemic GC administration on neurodevelopment. The first choice of GCs to minimize the adverse effects on the developing brain is still under debate. We investigated the effect of commonly used GCs such as dexamethasone (DEX), betamethasone (BET) and hydrocortisone (HDC) on the proliferation of human-induced pluripotent stem cell (iPSC)-derived neuronal progenitor cells (NPCs). In this study, NPCs were treated with various concentrations of GCs and subjected to cell proliferation assays. Furthermore, we quantified the number of microtubule-associated protein 2 (MAP2) positive neurons in NPCs by immunostaining. All GCs promoted NPC proliferation in a dose-dependent manner. We also confirmed that MAP2-positive neurons in NPCs increased upon GC treatment. However, differential effects of GCs on MAP2 positive neurons were observed when we treated NPCs with H_2O_2. The total numbers of NPCs increased upon any GC treatment even under oxidative conditions but the numbers of MAP2 positive neurons increased only by HDC treatment. GCs promoted human iPSCs–derived NPC proliferation and the differential effects of GCs became apparent under oxidative stress. Our results may support HDC as the preferred choice over DEX and BET to prevent adverse effects on the developing human brain.

Keywords: Glucocorticoids; Neural progenitor cell; iPSC; Cell culture; Proliferation

Introduction

In recent years, systemic glucocorticoids (GCs) have frequently been administered to treat and prevent chronic lung disease (CLD), which is also known as bronchopulmonary dysplasia, and circulatory dysfunction in premature infants. GCs administration dramatically improves the outcome of premature infants with established CLD (Halliday et al. 2009, 2010). However, the use of GCs, especially dexamethasone (DEX), for CLD patients is reported to show detrimental effects on the developing brain with subsequent behavioral alterations and cerebral palsy (Murphy et al. 2001; Shinwell et al. 2000; Yeh et al. 2004). Betamethasone (BET) is also reported to impair cerebral blood flow velocities in very premature infants with severe CLD (Cambonie et al. 2008). A few studies have suggested that patients treated with HDC showed no neurological adverse effect (Benders et al. 2009; de Jong et al. 2011; Watterberg et al. 2007), but another study showed that GCs reduced proliferation and induce differentiation of neurons (Aden et al. 2011). The effect of GCs on the developing human brain remains elusive, and randomized clinical trials are required in order to establish better neurological outcomes.

Many studies have been conducted to reveal the mechanisms underlying the adverse effects of GCs. DEX treatment has been shown to decrease brain weight (Kanagawa et al. 2006) and inhibit hippocampal neurogenesis (Kim et al. 2004) in rats. In addition, DEX inhibited the proliferation of embryonic rat neural stem cells (Bose et al. 2010). Duksal et al. (2009) reported that high dose DEX caused brain weight loss due to neuronal apoptosis. Although many animal studies have indicated that GCs suppress the

* Correspondence: shintaku@med.osaka-cu.ac.jp
[1]Department of Pediatrics, Osaka City University Graduate School of Medicine, 1-4-3 Asahi-machi, Abeno-ku, Osaka 545-8585, Japan
Full list of author information is available at the end of the article

proliferation of neuronal cells, it remains unknown how GCs affect neuronal cells in humans.

In the present study, we investigated the effects of commonly used GCs such as DEX, BET and HDC on the proliferation of human iPS cell-derived NPCs, which were used as a model of human embryonic and neonatal NPCs. We further focused on the subpopulation of NPCs that were committed to the neuronal lineage. The effects of GCs on neural cell proliferation were evaluated. We also examined whether oxidative stress affected the sensitivity of NPCs to GCs.

Methods

Reagents

DECADRON® (Dexamethasone) was obtained from MSD (Tokyo, Japan). Rinderon® (Betamethasone) was from Shionogi & Co., Ltd. (Osaka, Japan). Hydrocortone® (hydrocortisone) was from Nichi-Iko Pharmaceutical Co., Ltd. (Toyama, Japan). Hydrogen peroxide solution (H_2O_2) was from Wako Pure Chemical Industries, Ltd. (Osaka, Japan).

Human iPS cell culture and neural progenitor cells induction

The study was approved by the Ethics Committees of the Osaka City University (approval #2472) and was conducted according to the declaration of Helsinki. In this study, we used human iPSCs derived from fetal lung fibroblast (MRC-5) cells and the iPSCs were maintained by standard culture methods as described previously (Saito et al. 2011). Neural induction was performed as described previously (Chambers et al. 2009). Briefly, neural induction will be initiated by 10 μM SB431542 (TGF-β inhibitor, Wako) and 200 ng/ml of Noggin (R&D Systems, Minneapolis, MN). After 8 days of neural induction, cells are dissociated with accutase (Chemicon, Temecula, CA) and plated onto poly-ornithine and laminin (Sigma, St. Louis, MO) with neurobasal medium supplemented with 2% B27 (Invitrogen), 20 ng/ml bFGF (Wako), 20 ng/ml epidermal growth factor (EGF, Invitrogen). Rosette neural stem cells (R-NSC) will form within a few days. R-NSCs were enriched by Neural Rosette Selection Reagent® (Stem Cell Technologies, Toronto, Canada). NPCs were obtained after a few passages and subjected to proliferation assays. Schematic diagram of induction of NPCs and representative growth rate of NPCs are shown in Additional file 1: Figure S1.

Proliferation assay

Cell proliferation was measured using Cell Titer 96 AQueous One Solution cell proliferation assay according to the manufacturer's protocol (Promega, Madison, WI). Ninety-six-well tissue culture plates were coated with poly-ornithine and laminin. NPCs were plated at a density of 6×10^3 cells per well. GCs treatment was started 48 h after plating. After 4 days of GCs exposure, proliferation assays was performed by adding Cell Titer 96 AQueous One Solution and incubating at 37°C for 2 h. Then absorbance was measured at 450 nm with a micro plate reader (MTP-300:CORONA ELECTRIC).

Immunocytochemistry and MAP2 positive cell count

Chamber slides, μ-slide IV (Ibidi, Martinsried, Germany) were coated with poly-ornithine and laminin. NPCs were plated in the chamber slides at a density of 1.8×10^4 cells per well and cultured for 48 h, followed by exposure to GCs. After 4 days incubation, cells were subjected for immunostaining. Mouse monoclonal anti-MAP2 antibody (AP20) (Chemicon, Temecula, CA) (1:200), Alexa Fluor® 488 Goat Anti-Mouse IgG (Invitrogen) (1:1000), and 4,6-diamidino-2-phenylindole (DAPI) (Sigma) were used. For quantification of MAP2 positive cells and DAPI positive cells, 5 microscopic fields were randomly selected and cells were automatically counted using ImageJ (Schneider et al. 2012). Cell counts per field were standardized against untreated cell counts for each experiment.

Statistical analysis

For statistical analysis, data were evaluated by analysis of variance (Statcel3, add-in software to Microsoft® Excel 2007). Differences between groups were analyzed by single-factor ANOVA with Tukey-Kramer. Results are displayed with mean ± SD. P values < 0.05 were considered statistically significant. All experiments were repeated more than three times.

Results

GC treatment promoted neural progenitor cell proliferation

To evaluate the effect of GCs on the proliferation of NPCs, we initially performed a cell proliferation assay. NPCs were exposed to GCs for 4 days and subjected to a proliferation assay. As shown in Figure 1a, the average absorbance of the samples treated with DEX of 5 nM, 500 nM, and 50 μM were 107.5 ± 10.2 (P value = NS), 113.8 ± 17.1 (P value < 0.05), and 124.0 ± 8.9 (P value < 0.01), respectively. The samples treated with BET of 5 nM, 500 nM, and 50 μM were 108.7 ± 9.8 (P value = NS), 110.2 ± 12.4 (P value = NS), and 114.4 ± 9.4 (P value < 0.01), respectively (Figure 1b). The samples treated with HDC of 5 nM, 500 nM, and 50 μM were 105.0 ± 8.6 (P value = NS), 114.0 ± 11.3 (P value < 0.01), and 118.4 ± 9.3 (P value < 0.01), respectively (Figure 1c). We also calculated the P values for comparison of each GC from 5 nM to 50 μM. Both DEX and HDC showed statistically significant differences on the absorbance between 5 nM and 50 μM (P value < 0.01).

In summary, our results indicate that the GCs stimulate proliferation of NPCs in a dose-dependent manner. Moreover, the proliferative effect was independent from the types of GCs we tested.

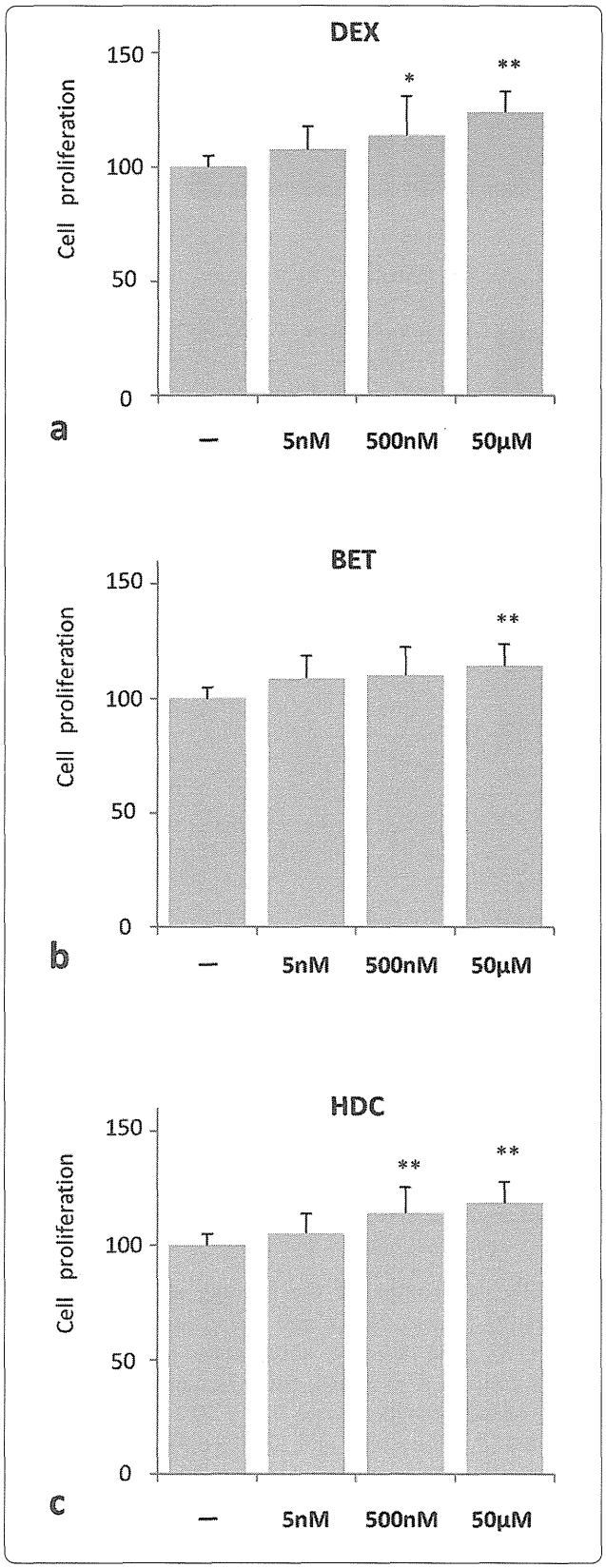

Figure 1 Glucocorticoid (GC) treatment promoted NPC proliferation. Cell proliferation was measured by absorbance using Cell 96 AQueous One Assay kit. The average absorbance data were expressed as percentages of untreated samples. *P* values were calculated by comparing with untreated samples (n = 3). $*P < 0.05$, $**P < 0.01$. (One-way ANOVA with Tukey-Kramer). The cells were treated with the indicated concentration of **(a)** dexamethasone (DEX), **(b)** betamethasone (BET), and **(c)** hydrocortisone (HDC).

GC treatment promoted cell proliferation of MAP2 positive neuron

GC treatment is reported to increase apoptosis in distinct neural regions in the brain. The studies indicate that neuronal cells are more susceptible than glial cells (Duksal et al. 2009; Hassan et al. 1996). Since iPS cell-derived NPCs consist of heterogeneous populations, we focused on proliferation of the cells that were committed to the neuronal lineage in the GC-treated NPCs.

Microtubule-associated protein 2 (MAP2) is specifically expressed *in vivo* in the granular layer in the embryo (Tucker et al. 1989). We performed immunostaining using an anti-MAP2 antibody to evaluate the number of neuronal lineage cells after GC treatments (Figure 2c). For this experiment, NPCs were exposed to GCs for 4 days and then subjected to analysis.

We compared the MAP2 positive cell count with the untreated NPCs and calculated the *P* values. As shown in Figure 2b, the average numbers of MAP2-positive neurons treated with DEX of 500 nM and 50 μM were 125.4 ± 36.0 (*P* value < 0.05) and 158.6 ± 35.3 (*P* value < 0.01), respectively. The MAP2-positive neurons treated with BET of 500 nM and 50 μM were 122.7 ± 36.0 (*P* value = NS) and 173.0 ± 39.6 (*P* value < 0.01), respectively (Figure 2c). The MAP2-positive neurons treated with HDC of 500 nM and 50 μM were 116.0 ± 26.1 (*P* value = NS) and 145.1 ± 36.7 (*P* value < 0.01), respectively (Figure 2d). All GCs showed statistically significant differences on the average numbers of MAP2-positive neurons between 5 nM and 50 μM (DEX and HDC showed *P* value < 0.05, BET showed *P* value < 0.01). These data indicate that the MAP2 positive cell number significantly increased as the cells were treated with a higher dose of GCs. Moreover, we found no significant differences in proliferative potency between DEX, BET, and HDC.

GC treatment promoted NPC proliferation under oxidative stress

Involvement of oxidative stress was suggested in the pathogenesis of neonatal CLD (Ogihara et al. 1999) and oxidative stress is thought to be a cause of neuronal damage (Ikonomidou and Kaindl 2011). To mimic clinical situations during the use of GCs, we treated NPCs with H_2O_2 for oxidative stress and examined the effect of GCs on NPC proliferation. We have initially tested

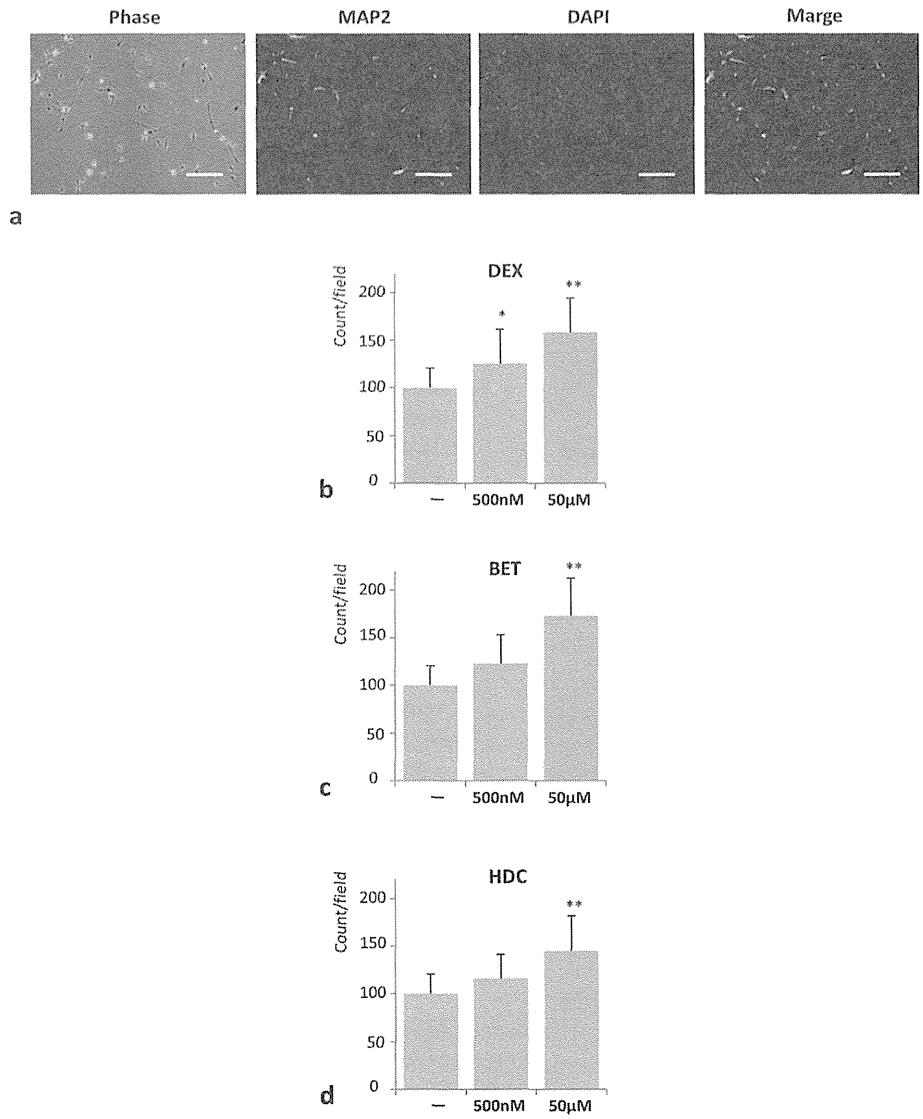

Figure 2 GC treatment promoted cell proliferation of MAP2 positive neurons. (a) Representative pictures of NPCs stained with an antibody against MAP2 (red) and nuclear counterstain DAPI (blue). Phase, phase contrast image. Scale bar, 100 μm. **(b-d)**. Quantification of MAP2 positive neurons using ImageJ. *P* values were calculated by comparing GC treated with untreated samples (n = 3). $*P < 0.05$, $**P < 0.01$. (One-way ANOVA with Tukey-Kramer). The cells were treated with the indicated concentration of **(b)** dexamethasone (DEX), **(c)** betamethasone (BET), and **(d)** hydrocortisone (HDC).

various concentration of H2O2 on the NPCs without GCs. 300 μM H2O2 concentration was reasonably seen the effect of the stress on cellular proliferation (Additional file 2: Figure S2).

NPCs were treated with 300 μM H_2O_2 1 day before GC treatment. Similarly, we expressed the average absorbance data as percentages of untreated samples, and the mean percent ± SD of untreated samples was 100 ± 5.0. The results are shown in Figure 3. The average absorbance of cells that were treated only with H_2O_2 was 88.8 ± 7.8, which is significantly reduced relative to the untreated samples (*P* value < 0.05, Figure 3).

Initially, we compared the average absorbance with only H_2O_2 treated NPCs and calculated the *P* values (Figure 3). The average absorbance of the samples treated with DEX of 5 nM, 500 nM, and 50 μM under H_2O_2-treated condition were 93.8 ± 10.3 (*P* value = NS), 96.6 ± 8.0 (*P* value = NS), and 124.0 ± 6.9 (*P* value < 0.01), respectively. The average absorbance of cells treated with BET of 5 nM, 500 nM, and 50 μM under H_2O_2-treated condition were 96.0 ± 8.6 (*P* value = NS), 103.2 ± 7.6 (*P* value < 0.01), and 109.4 ± 2.9 (*P* value < 0.01), respectively. The average absorbance of cells treated with HDC of 5 nM, 500 nM, and 50 μM under H_2O_2-treated

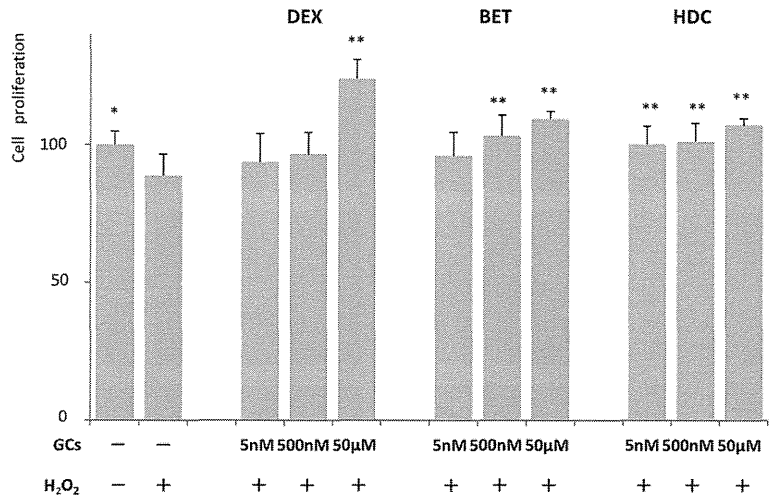

Figure 3 GC treatment promoted NPC proliferation under oxidative stress. Cell proliferation was measured by absorbance using Cell 96 AQueous One Assay kit. The average absorbance data were expressed as percentages of untreated samples. *P* values were calculated by comparing GC treated with untreated samples (n = 3). **P* < 0.05, ***P* < 0.01. (One-way ANOVA with Tukey-Kramer). DEX: dexamethasone, BET: betamethasone, HDC: hydrocortisone.

condition were 100.2 ± 6.6 (*P* value < 0.01), 101.2 ± 6.8 (*P* value < 0.01), and 107.2 ± 2.5 (*P* value < 0.01), respectively. When we compared the average absorbance between each GC in the same concentration with or without H_2O_2, we did not observe statistical significance except for DEX at 5 nM and 500 nM (*P* value < 0.01). These data indicate that the absorbance significantly increased as the cells were treated with a higher dose of GCs even under H_2O_2-treated condition.

In summary, our results indicate that GCs stimulated the proliferation of NPCs under H_2O_2-treated conditions. All examined GCs induced NPC proliferation in a dose dependent manner regardless of oxidative stress.

HDC alone promoted cell proliferation of MAP2 positive neuron under oxidative stress

Neurons are more sensitive to oxidative stress than any other type of cells in the brain (Hayashi et al. 2012). Therefore, we examined the effects of the GCs on the proliferation of MAP2-positive neurons under an oxidative stress condition. NPCs were treated with 300 μM H_2O_2 1 day before GC treatment, then NPCs were exposed to GCs for 4 days and subjected to immunostaining using an anti-MAP2 antibody (Figure 4a).

We compared the MAP2 positive cell count with the condition treated with H_2O_2 alone (74.9 ± 31.8). The average numbers of MAP2-positive neurons treated with DEX of 500 nM and 50 μM were 75.6 ± 52.3 (*P* value = NS) and 84.7 ± 27.2 (*P* value = NS), respectively. The average numbers of MAP2-positive neurons treated with BET of 500 nM and 50 μM were 93.1 ± 41.1 (*P* value = NS) and 113.1 ± 47.7 (*P* value = NS), respectively. The average numbers of MAP2-positive neurons treated with HDC of 500 nM and 50 μM were 108.5 ± 34.0 (*P* value < 0.05) and 143.6 ± 19.4 (*P* value < 0.01), respectively. Unlike DEX and BET, HDC significantly increased the number of MAP2-positive neurons compared with the untreated samples even under the H_2O_2-treated condition.

In conclusion, only HDC promoted significant cell proliferation of MAP2 positive neurons as well as the total number of NPCs under oxidative stress. DEX and BET, however, increased the total number of NPCs without increasing MAP2 positive neurons.

Discussion

In this study, we investigated the effect of GCs on proliferation of NPCs derived from human iPS cells. Unexpectedly, all GCs we tested induced NPC proliferation in a dose dependent manner. We also confirmed that MAP2 positive neuronal cells were increased by GC treatment. Furthermore, we investigated the proliferative effects of GCs under an oxidative stress condition that could be more relevant to the clinical setting. The findings revealed that all GCs stimulated the total number of NPCs even under the oxidative condition, but MAP2 positive neurons were only increased by HDC treatment. Our results support the finding that HDC would be the preferred choice over DEX and BET to prevent adverse effects on the developing brain.

Cell cycle regulation induced by GCs

Samarasinghe et al. (Samarasinghe et al., 2011) demonstrated that the binding of GCs to the GC receptor (GR) decreased gap junction-mediated intercellular

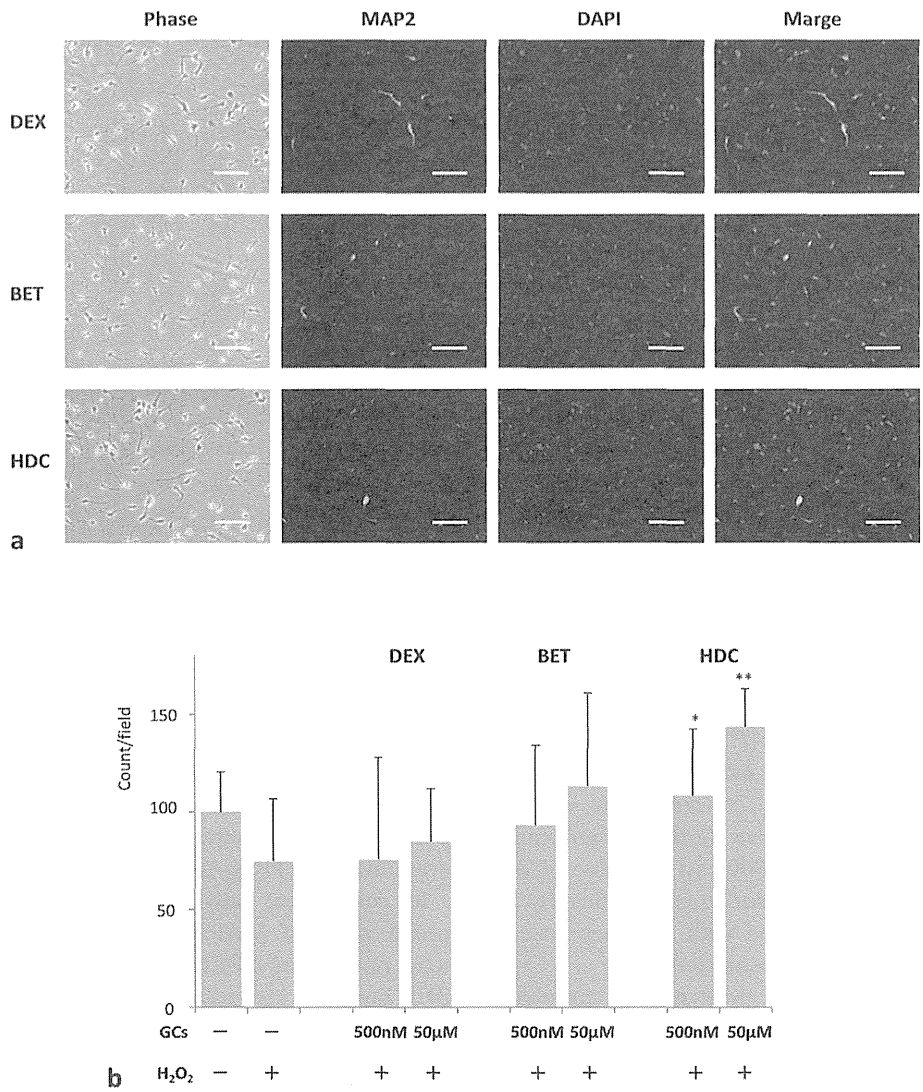

Figure 4 GCs showed different effects on proliferation of the MAP2-positive neurons under H_2O_2-treated conditions. (a) Representative pictures of NPCs were stained with an antibody against MAP2 (red) and nuclear counterstain DAPI (blue). The cells were pre-exposed to H_2O_2 and treated with 50 μM of the indicated GCs. Phase, phase contrast image. Scale bar, 100 μm. **(b)** Quantification of MAP2 positive neurons using ImageJ. *P* values were calculated by comparing GC treated samples with the samples treated with H_2O_2 alone (n = 3). $^{*}P < 0.05$, $^{**}P < 0.01$. (One-way ANOVA with Tukey-Kramer). DEX: dexamethasone, BET: betamethasone, HDC: hydrocortisone. Note that HDC alone promoted significant cell proliferation of MAP2 positive neurons under oxidative stress.

communication and led to a decrease in the rate of cells in the S phase. They concluded that GC suppresses cell proliferation through this mechanism. Sundberg et al. (2006) reported that the activation of GR prevents cyclin D1-mediated cell cycle progression and that the high dose GC inhibits proliferation of rat embryonic NPCs. Similar inhibitory mechanisms of GCs were reported by others using rodent cells (Bose et al. 2010). Moors et al. (2012) examined the effect of DEX on neurospheres derived from a 16-week human aborted fetus and found that DEX inhibits the proliferation of human NPCs. However, in our experiment using NPCs derived from human iPS cells, all GCs we tested including DEX intriguingly promoted the proliferation of NPCs.

Neuroprotective effects of GCs

GCs exhibit protective effects on postmitotic neurons. Harms et al. (2007) showed that GCs induce phosphatidylinositol 3-Akt-kinase-dependent phosphorylation of p21Waf1/Cip1 and it works as a novel anti-apoptotic pathway for postmitotic primary cortical neurons isolated from rats and mice. By *in vivo* and *in vitro* studies using the rat model, Jeanneteau et al. (2008) showed that GCs activate the Trk neurotrophin receptor and thus exhibit

neuroprotective effects. In any case, neuroprotective pathways in postmitotic neurons prevent new cell cycles. Therefore, such a neuroprotective mechanism alone cannot explain how GCs induce NPC proliferation.

Differential mechanisms of action between GCs

We demonstrated that GCs differently stimulate the proliferation of MAP2-positive neurons under oxidative stress. HDC physically associates with both GR and mineralcorticoid receptor (MR) *in vivo,* while DEX and BET physically associate only with GR but not with MR (De Kloet et al. 1998). As described above, it has been reported that GR suppresses cell proliferation and causes apoptosis. In the present study, the GCs showed similar effects under non-stressed conditions. Under oxidative stress conditions, however, HDC alone increased the number of MAP2 positive neurons. This may suggest that the activation of MR plays an important role in the proliferation of neurons under oxidative stress. Another possibility could be the difference in the inactivation mechanisms of the GCs. While HDC is metabolized by 11βHSD2, DEX and BET are not sensitive to inactivation by 11βHSD2 (Heine and Rowitch 2009; Noguchi et al. 2011). Thus, the continuous GR activity may induce apoptosis under stress conditions. The human NPCs used in this study were indeed expressing both MR and GR (Additional file 3: Figure S3).

Clinical implications

Our current study demonstrates that NPCs proliferate in response to GCs but MAP2 positive neurons are sensitive to oxidative stress. It is interesting that the response to HDC is less affected by oxidative stress than DEX or BET (Figure 4). Halliday et al. (2009, 2010) recommended avoiding frequent use of GCs for CLD treatment but there is insufficient evidence regarding which types of GCs to use in order to minimize adverse neurological outcomes. Further clinical and mechanistic studies are required to determine the optimal choice of GCs for children with CLD.

In conclusion, we evaluated the effect of GCs on NPC derived human iPS cells and found unique proliferative effects on NPCs, which were altered by external stress. Further mechanistic studies are needed to reveal how GCs induce NPC proliferation and how oxidative stress modulates the effects of GCs.

Additional files

Additional file 1: Figure S1. Derivation of neural progenitor cells (NPCs) from human iPS cells. (a) Schematic diagram of induction of NPCs. R-NSC: Rosette neural stem cells. (b) Representative picture of R-NSC and NPCs in phase contrast image. R-NSC stained positive for Nestin (green/insert). Bar:100 μm. (c) Growth curve for NPCs. Cell number was automatically measured by using IncuCyte imaging system (Essen BioScience, K.K., Japan).

Additional file 2: Figure S2. Effect of H_2O_2 treatment on NPC proliferation under oxidative stress. NPCs were treated various concentration of H_2O_2 as indicated. Cell proliferation was measured by absorbance using Cell 96 AQueous One Assay kit. The average absorbance data were expressed as percentages of untreated samples.

Additional file 3: Figure S3. Expression of glucocorticoid receptor and mineral corticoid receptor in NPCs Quantitative RT-PCR analysis was performed on MRC5-iPSC and NPCs. The mRNA values were expressed relative to the control gene (β-actin). GR: glucocorticoid receptor, MR: mineral corticoid receptor.

Competing interests

The authors declare that they have no competing interests.

Authors' contributions

EN, TH, TH carried out the cell culture studies, and drafted the manuscript. MT, AU provided materials and conceived of the study. HS participated in study design, coordination and helped to draft the manuscript. All authors read and approved the final manuscript.

Acknowledgments

We thank Dr Katherine E Santostefano (University of Florida) for helpful discussion and critical readings of the manuscript. This work was supported by the Japanese Ministry of Education, Culture, Sports, Science, and Technology (TH and HS) and Takeda Science Foundation (TH).

Author details

[1]Department of Pediatrics, Osaka City University Graduate School of Medicine, 1-4-3 Asahi-machi, Abeno-ku, Osaka 545-8585, Japan. [2]Research Team for Geriatric Medicine (Vascular Medicine), Tokyo Metropolitan Institute of Gerontology, Sakaecho 35-2, Itabashi-Ku, Tokyo 173-0015, Japan. [3]Department of Reproductive Biology, National Research Institute for Child Health and Development, 2-10-1 Ookura, Setagaya-ku, Tokyo 157-8535, Japan.

Received: 25 July 2014 Accepted: 6 September 2014
Published: 15 September 2014

References

Aden P, Paulsen RE, Maehlen J, Loberg EM, Goverud IL, Liestol K, Lomo J (2011) Glucocorticoids dexamethasone and hydrocortisone inhibit proliferation and accelerate maturation of chicken cerebellar granule neurons. Brain Res 1418:32–41

Benders MJ, Groenendaal F, van Bel F, Ha Vinh R, Dubois J, Lazeyras F, Warfield SK, Huppi PS, de Vries LS (2009) Brain development of the preterm neonate after neonatal hydrocortisone treatment for chronic lung disease. Pediatr Res 66:555–559

Bose R, Moors M, Tofighi R, Cascante A, Hermanson O, Ceccatelli S (2010) Glucocorticoids induce long-lasting effects in neural stem cells resulting in senescence-related alterations. Cell Death Dis 1:e92

Cambonie G, Mesnage R, Milesi C, Pidoux O, Veyrac C, Picaud JC (2008) Betamethasone impairs cerebral blood flow velocities in very premature infants with severe chronic lung disease. J Pediatr 152:270–275

Chambers SM, Fasano CA, Papapetrou EP, Tomishima M, Sadelain M, Studer L (2009) Highly efficient neural conversion of human ES and iPS cells by dual inhibition of SMAD signaling. Nat Biotechnol 27:275–280

de Jong SE, Groenendaal F, van Bel F, Rademaker KJ (2011) Pulmonary effects of neonatal hydrocortisone treatment in ventilator-dependent preterm infants. Int J Pediatr 2011:783893

De Kloet ER, Vreugdenhil E, Oitzl MS, Joels M (1998) Brain corticosteroid receptor balance in health and disease. Endocr Rev 19:269–301

Duksal F, Kilic I, Tufan AC, Akdogan I (2009) Effects of different corticosteroids on the brain weight and hippocampal neuronal loss in rats. Brain Res 1250:75–80

Halliday HL, Ehrenkranz RA, Doyle LW (2009) Late (>7 days) postnatal corticosteroids for chronic lung disease in preterm infants. Cochrane Database Syst Rev (1):CD001145, doi:10.1002/14651858.CD001145.pub2

Halliday HL, Ehrenkranz RA, Doyle LW (2010) Early (<8 days) postnatal corticosteroids for preventing chronic lung disease in preterm infants. Cochrane Database Syst Rev (1):CD001146, doi:10.1002/14651858.CD001145.pub3

Harms C, Albrecht K, Harms U, Seidel K, Hauck L, Baldinger T, Hubner D, Kronenberg G, An J, Ruscher K, Meisel A, Dirnagl U, von Harsdorf R,

Endres M, Hortnagl H (2007) Phosphatidylinositol 3-Akt-kinase-dependent phosphorylation of p21(Waf1/Cip1) as a novel mechanism of neuroprotection by glucocorticoids. In J Neurosci 27:4562–4571

Hassan AH, von Rosenstiel P, Patchev VK, Holsboer F, Almeida OF (1996) Exacerbation of apoptosis in the dentate gyrus of the aged rat by dexamethasone and the protective role of corticosterone. In Exp Neurol 140:43–52

Hayashi M, Miyata R, Tanuma N (2012) Oxidative stress in developmental brain disorders. Adv Exp Med Biol 724:278–290

Heine VM, Rowitch DH (2009) Hedgehog signaling has a protective effect in glucocorticoid-induced mouse neonatal brain injury through an 11betaHSD2-dependent mechanism. J Clin Invest 119:267–277

Ikonomidou C, Kaindl AM (2011) Neuronal death and oxidative stress in the developing brain. Antioxid Redox Signal 14:1535–1550

Jeanneteau F, Garabedian MJ, Chao MV (2008) Activation of Trk neurotrophin receptors by glucocorticoids provides a neuroprotective effect. Proc Natl Acad Sci U S A 105:4862–4867

Kanagawa T, Tomimatsu T, Hayashi S, Shioji M, Fukuda H, Shimoya K, Murata Y (2006) The effects of repeated corticosteroid administration on the neurogenesis in the neonatal rat. Am J Obstet Gynecol 194:231–238

Kim JB, Ju JY, Kim JH, Kim TY, Yang BH, Lee YS, Son H (2004) Dexamethasone inhibits proliferation of adult hippocampal neurogenesis *in vivo* and *in vitro*. Brain Res 1027:1–10

Moors M, Bose R, Johansson-Haque K, Edoff K, Okret S, Ceccatelli S (2012) Dickkopf 1 mediates glucocorticoid-induced changes in human neural progenitor cell proliferation and differentiation. In Toxicol Sci 125:488–495

Murphy BP, Inder TE, Huppi PS, Warfield S, Zientara GP, Kikinis R, Jolesz FA, Volpe JJ (2001) Impaired cerebral cortical gray matter growth after treatment with dexamethasone for neonatal chronic lung disease. Pediatrics 107:217–221

Noguchi KK, Lau K, Smith DJ, Swiney BS, Farber NB (2011) Glucocorticoid receptor stimulation and the regulation of neonatal cerebellar neural progenitor cell apoptosis. Neurobiol Dis 43:356–363

Ogihara T, Hirano K, Morinobu T, Kim HS, Hiroi M, Ogihara H, Tamai H (1999) Raised concentrations of aldehyde lipid peroxidation products in premature infants with chronic lung disease. Arch Dis Child Fetal Neonatal Ed 80:21–25

Saito S, Onuma Y, Ito Y, Tateno H, Toyoda M, Hidenori A, Nishino K, Chikazawa E, Fukawatase Y, Miyagawa Y, Okita H, Kiyokawa N, Shimma Y, Umezawa A, Hirabayashi J, Horimoto K, Asashima M (2011) Possible linkages between the inner and outer cellular states of human induced pluripotent stem cells. BMC Syst Biol 5(Suppl 1):S17

Samarasinghe RA, Di Maio R, Volonte D, Galbiati F, Lewis M, Romero G, DeFranco DB (2011) Nongenomic glucocorticoid receptor action regulates gap junction intercellular communication and neural progenitor cell proliferation. Proc Natl Acad Sci U S A 108:16657–16662

Schneider CA, Rasband WS, Eliceiri KW (2012) NIH Image to ImageJ: 25 years of image analysis. Nat Methods 9:671–675

Shinwell ES, Karplus M, Reich D, Weintraub Z, Blazer S, Bader D, Yurman S, Dolfin T, Kogan A, Dollberg S, Arbel E, Goldberg M, Gur I, Naor N, Sirota L, Mogilner S, Zaritsky A, Barak M, Gottfried E (2000) Early postnatal dexamethasone treatment and increased incidence of cerebral palsy. Arch Dis Child Fetal Neonatal Ed 83:177–181

Sundberg M, Savola S, Hienola A, Korhonen L, Lindholm D (2006) Glucocorticoid hormones decrease proliferation of embryonic neural stem cells through ubiquitin-mediated degradation of cyclin D1. In J Neurosci 26:5402–5410

Tucker RP, Garner CC, Matus A (1989) In situ localization of microtubule-associated protein mRNA in the developing and adult rat brain. Neuron 2:1245–1256

Watterberg KL, Shaffer ML, Mishefske MJ, Leach CL, Mammel MC, Couser RJ, Abbasi S, Cole CH, Aucott SW, Thilo EH, Rozycki HJ, Lacy CB (2007) Growth and neurodevelopmental outcomes after early low-dose hydrocortisone treatment in extremely low birth weight infants. Pediatrics 120:40–48

Yeh TF, Lin YJ, Lin HC, Huang CC, Hsieh WS, Lin CH, Tsai CH (2004) Outcomes at school age after postnatal dexamethasone therapy for lung disease of prematurity. N Engl J Med 350:1304–1313

doi:10.1186/2193-1801-3-527
Cite this article as: Ninomiya *et al.*: Glucocorticoids promote neural progenitor cell proliferation derived from human induced pluripotent stem cells. *SpringerPlus* 2014 3:527.

Sapropterin Is Safe and Effective in Patients less than 4-Years-Old with BH_4-Responsive Phenylalanine Hydroxylase Deficiency

Haruo Shintaku, MD, PhD[1], and Toshihiro Ohura, MD, PhD[2]

Objective To assess the safety and efficacy of tetrahydrobiopterin therapy with sapropterin to treat tetrahydrobiopterin (BH_4)-responsive phenylalanine hydroxylase (PAH) deficiency in children aged <4 years compared with those aged ≥4 years.

Study design We analyzed a longitudinal follow-up study conducted in all patients with BH_4-responsive PAH deficiency throughout Japan. At the end of 2011, 43 patients were receiving sapropterin, of whom 21 were aged <4 years at the initiation of treatment. The starting dose of sapropterin was ≥10 mg/kg/day in 11 of these 21 patients. The duration of follow-up was ≥4 years in 6 of those 11 patients; 3 of these 6 were followed for ≥10 years. Nine patients were receiving sapropterin monotherapy at the end of 2011.

Results Serum phenylalanine level was maintained within the recommended optimal control range in all 21 patients who started sapropterin treatment before age 4 years. Only 1 nonserious adverse drug reaction occurred, an elevated alanine aminotransferase level in 1 patient. No significant abnormal behavior related to nerve disorders was reported.

Conclusion Sapropterin therapy initiated before age 4 years was effective in maintaining serum phenylalanine level within the favorable range and was safe in Japanese patients with BH_4-responsive PAH deficiency. *(J Pediatr 2014;165:1241-4).*

Based on clinical trial data, sapropterin dihydrochloride, a tetrahydrobiopterin (BH_4) drug, has been approved for the treatment of BH_4-responsive phenylalanine hydroxylase (PAH) deficiency in patients aged ≥4 years in the US. Since the drug's approval, however, many patients aged <4 years have been treated with sapropterin. In Japan, sapropterin dihydrochloride granules 2.5% (Biopten, Daiichi Sankyo, Japan) was approved in 1992 for treatment of BH_4 deficiency and in 2008 for treatment of BH_4-responsive PAH deficiency.

We previously reported the safety and efficacy of long-term (16 years) treatment with sapropterin in BH_4-deficient patients who started treatment before age 4 years based on postmarketing surveillance in Japan.[1] Here we report on the long-term safety and efficacy of sapropterin in patients with BH_4-responsive PAH deficiency who started treatment before age 4 years.

Methods

At the end of 2011, 43 patients in Japan were receiving BH_4 therapy with sapropterin, 21 of whom were aged <4 years at the start of treatment. Only 1 patient aged ≥4 years was hospitalized. One child aged <4 years and 6 children aged ≥4 years had a BH_4-responsive sibling. All patients had undergone neonatal phenylketonuria screening and pteridine analysis, along with a dihydropteridine reductase assay that identified them as not BH_4-deficient.[2]

The present postmarketing surveillance study was conducted in 21 medical centers in Japan between 1995 and 2011. During this period, serum phenylalanine (Phe) concentrations were measured using an automated amino acid analyzer (L-8800; Hitachi, Tokyo, Japan), and serum pteridine concentrations were measured by high-performance liquid chromatography (LC-10; Shimazu, Kyoto, Japan) after iodine oxidation. Dihydropteridine reductase activity was measured using Guthrie card specimens, as described previously.[2]

A 1-week loading test (20 mg/kg/day in 2 doses for 7 consecutive days) was performed to evaluate BH_4 responsiveness. A 30% decrease in Phe level was defined as BH_4-responsive hyperphenylalaninemia.

Results

The clinical characteristics of the study patients and serum Phe levels before sapropterin treatment are presented in **Table I**. The study cohort comprised 21

BH_4	Tetrahydrobiopterin
PAH	Phenylalanine hydroxylase
Phe	Phenylalanine

From the [1]Department of Pediatrics, Osaka City University School of Medicine, Osaka, Japan; and [2]Department of Pediatrics, Tohoku University School of Medicine, Sendai, Japan

Supported by the Ministry of Health, Labour and Welfare, Japan (grant 14427732 to H.S. to produce the manuscript). H.S. received the data of postmarketing surveillance of Biopten for BH_4-responsive hyperphenylalaninemia. H.S. and T.O. received consultant, travel, and lecture fees from Daiichi Sankyo. The authors declare no conflict of interest.

Portions of the study were presented as a poster at International Congress of Inborn Errors of Metabolism, Barcelona, Spain, September 4, 2013.

http://dx.doi.org/10.1016/j.jpeds.2014.08.003

Table I. Patient characteristics, serum Phe level before BH_4 treatment, and BH_4 duration and dose

Characteristics	Age at administration <4.0 y	Age at administration ≥4.0 y
Sex, n		
Male	10	12
Female	11	10
Age as of December 2011, y, n		
<1	1	0
1 to <4	9	0
4 to <10	8	9
10 to <16	2	12
>16	1	1
Age at administration, y, n		
<1	8	0
1 to <4	13	0
4 to <10	0	18
10 to <16	0	3
>16	0	1
Complications, n		
No	17	15
Yes	4	7
BH_4 combined with diet therapy (at the end of 2011)		
No	9	10
Yes	12	12
Treatment duration, y, n		
<1	2	3
1-3	13	18
4-6	1	0
7-10	2	0
>10	3	1
BH_4 dose, mg/kg, n		
<5	2 (3)*	2 (3)*
5 to <10	8 (7)*	11 (11)*
10 to <15	8 (7)*	5 (6)*
15 to <20	1 (3)*	3 (1)*
≥20	2 (1)*	1 (1)*
Serum Phe level before BH_4 treatment, μmol/L, mean ± SD (range)		
Mass screening (at 5 d after birth)	472.1 ± 149.5 (224.2-818.1)	667.8 ± 282.4 (242.4-1187.3)
First visit (at hospital visit for thorough checkup)	479.3 ± 214.0 (169.7-981.8)	673.0 ± 521.5 (66.7-2230.3)
Initial investigation (before BH_4-loading test)	280.0 ± 146.8 (78.8-757.6)	420.7 ± 272.0 (161.2-1266.7)

*Number of patients at initiation (at the end of 2011).

patients in whom treatment was initiated at age <4 years. The duration of treatment was ≥4 years in 6 of the 21 patients, ≥10 years in 3 of those 6 patients, and >16 years in 1 of the latter 3 patients.

Serum Phe levels were reduced in response to 3 different BH_4-loading tests. The average reduction in serum Phe level was 42.2% in the single-loading test, 42.0% in the 4-times loading test, and 55.4% in the 1-week loading test, with respective cutoff values of 20%, 30%, and 50%.[3] Based on these data, all 21 patients were diagnosed with BH_4-responsive PAH deficiency (**Figure 1**).

Phe level according to age at the end of 2011 are shown in **Figure 2**, in all patients and by age at treatment initiation (<4 years or ≥4 years). In 11 of the 21 patients who started sapropterin therapy before age 4 years, the initial dose was >10 mg/kg day (**Table I**). The duration of follow-up was >4 years in 6 of these 11 patients, and >10 years in 3 of the latter 6 patients (**Table I**). At the end of the study period, 9 of the 21 patients were receiving sapropterin monotherapy.

After 4 years of age all patients were treated with sapropterin. Serum Phe levels were maintained within a favorable range in both groups, with no significant difference between the groups (**Figure 2**). Serum Phe levels were maintained within a favorable range in the 21 patients who started treatment before age 4 years, but were variable (ranging from too low to too high) in the 22 patients who did so after age 4 years (**Figure 2**). However, there was no significant difference in mean Phe concentration before BH_4 therapy between the 2 age groups.

All patients responded to sapropterin treatment, showing reductions in serum Phe levels to within the recommended optimal control range. Among the 43 patients, 19 were treated with only sapropterin and 24 were treated with sapropterin plus diet therapy. The mean serum Phe levels was 368.4 μmol/L in the patients who received sapropterin monotherapy and 362.4 μmol/L in those who received sapropterin with diet therapy, a statistically nonsignificant difference ($P = .10$).

Examination of electroencephalograms performed in 7 patients revealed no abnormalities, and brain magnetic resonance imaging showed an abnormality in only 1 of 8 patients. Adverse events are reported in **Table II**. Only 1 nonserious adverse drug reaction occurred, a mild increase in alanine aminotransferase level that improved without the need to stop sapropterin therapy. All 21 patients have since developed normally, and all of those who have reached school age are now attending normal schools.

Discussion

Patients with BH_4-responsive PAH deficiency, many of whom carry the *R241C* allele, respond to BH_4 administration. Although no clear correlation was seen between the reduced serum Phe levels in the BH_4-loading tests and *PAH* gene mutations, at least 1 mild phenylketonuria mutation or missense mutation was found in patients with BH_4-responsive PAH deficiency.[3]

Notably, the duration of treatment was ≥4 years in 6 of the 21 patients, ≥10 years in 3 of those 6 patients, and >16 years in 1 of these latter 3 patients (who was treated for hyperphenylalaninemia without BH_4 deficiency). This study represents a unique long-term follow-up of patients with BH_4-responsive PAH deficiency. BH_4-responsive PAH deficiency was first reported by Kure et al[4] in 1999. All 43 patients with BH_4-responsive PAH deficiency in Japan have been treated with BH_4 therapy. Sapropterin was approved for treating BH_4 deficiency in 1992 in Japan.

Our findings show that the control of serum Phe level in patients with BH_4-responsive PAH deficiency is more even and effective when sapropterin treatment is initiated before age 4 years (**Figure 2**), although there was no significant difference in mean Phe level between the 2 age groups. In the patients who started treatment at age ≥4 years,

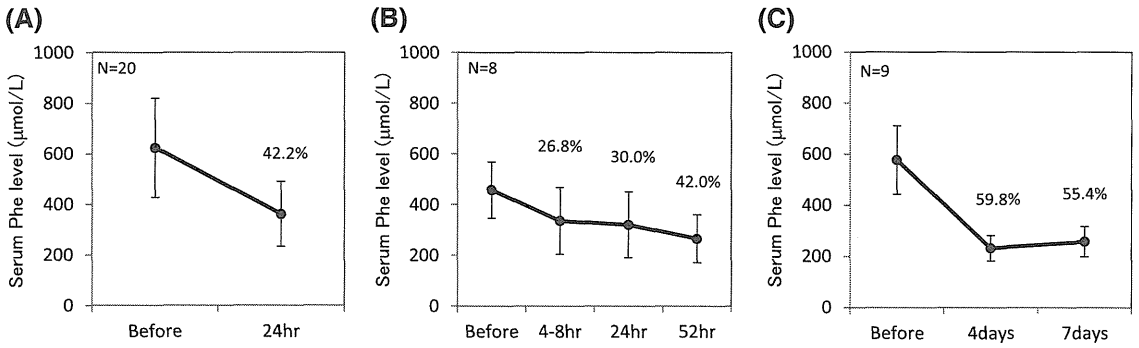

Figure 1. Serum Phe levels and response to BH_4-loading tests. **A,** Single loading test (cutoff, 20%). **B,** Four-times loading test (cutoff, 30%). **C,** One-week administration test (cutoff, 50%).

Phe levels varied more outside of the optimal range (**Figure** 2). Furthermore, during their first 4 years of life, it appears that Phe levels were better controlled within the optimal range by sapropterin therapy than by diet therapy, which can lower Phe levels to an excessive degree (**Figure** 2). At the end of this study, 19 of the 43 patients with BH_4-responsive PAH deficiency were treated with sapropterin monotherapy (**Table** I), and there was no significant difference in Phe level between the group treated with sapropterin monotherapy and the group treated with sapropterin plus diet therapy.

Sapropterin therapy is safe in this patient population, which is reassuring because treatment of BH_4-responsive PAH deficiency requires lifetime administration. Of the 21 patients who started treatment before age 4 years, 8 were aged <1 year, and treatment proved safe and effective in these children. No adverse side effects were reported, and there was no drug-related discontinuation of treatment.

Our safety results are supported by recent reports of sapropterin therapy in 147 patients with BH_4-responsive PAH deficiency with up to 12 years of follow-up in Europe that showed no severe adverse events; only 3 patients experienced adverse events, all of which disappeared when the dose was lowered.[5] Leuret et al[6] evaluated 15 patients under age 4 years who received sapropterin therapy and concluded, in agreement with our findings, that BH_4 therapy is efficient and safe before age 4 years in patients with BH_4-responsive PAH deficiency.

In the US, sapropterin was approved in 2007, and thus there is only 6 years of safety data on the use of this drug. In addition, the clinical trials for drug approval were conducted in children aged ≥4 years. Thus, the results of our study, with the longest follow-up reported to date, provide important assurance that long-term treatment with sapropterin is safe and effective in patients with BH_4-responsive PAH deficiency. ■

Submitted for publication Apr 5, 2014; last revision received Jul 8, 2014; accepted Aug 5, 2014.

Reprint requests: Haruo Shintaku, MD, PhD, Department of Pediatrics, Osaka City University Graduate School of Medicine, 1-4-3 Asahimachi, Abeno-ku, Osaka 545-8585, Japan. E-mail: shintakuh@med.osaka-cu.ac.jp

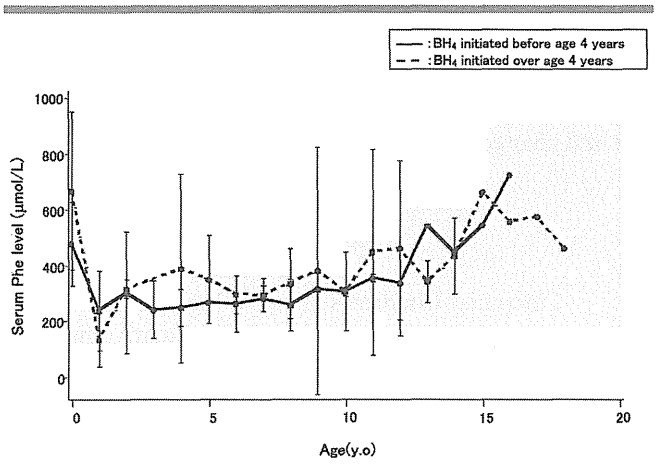

Figure 2. Phe levels according to patient age at treatment initiation and at the end of the study period. The *shaded area* indicates the recommended optimal control range.

Table II. Adverse events

Adverse events	Age at administration <4 y	Age at administration ≥4 y
All adverse events, n (%)	7 (33.3)	7 (31.8)
Infection and infestation, n (%)	5 (23.8)	4 (18.2)
Impetigo	0 (0.0)	1 (4.6)
Influenza	1 (4.8)	1 (4.6)
Nasopharyngitis	2 (9.5)	2 (9.1)
Adenoiditis	1 (4.8)	0 (0.0)
Varicella	1 (4.8)	1 (4.6)
Respiratory, thoracic, and mediastinal disorders, n (%)	3 (14.3)	3 (13.6)
Allergic rhinitis	0 (0.0)	2 (9.1)
Upper respiratory inflammation	3 (14.3)	2 (9.1)
Clinical blood test, n (%)	1 (4.8)	0 (0.0)
Alanine aminotransferase elevation*	1 (4.8)	0 (0.0)
Injury, poisoning, and procedural complications, n (%)	1 (4.8)	1 (4.6)
Clavicle fracture	0 (0.0)	1 (4.6)
Skin laceration	1 (4.8)	0 (0.0)

Multiple events occurred in 1 patient.
*Side effect (nonserious).

References

1. Shintaku H, Ohwada M. Long-term follow-up of tetrahydrobiopterin therapy in patients with tetrahydrobiopterin deficiency in Japan. Brain Dev 2013;35:406-10.
2. Shintaku H. Disorders of tetrahydrobiopterin metabolism and their treatment. Curr Drug Metab 2002;3:123-31.
3. Shintaku H, Kure S, Ohura T, Okano Y, Ohwada M, Sugiyama N, et al. Long-term treatment and diagnosis of tetrahydrobiopterinresponsive hyperphenylalaninemia with a mutant phenylalanine hydroxylase gene. Pediatr Res 2004;55:425-30.
4. Kure S, Hou DC, Ohura T, Iwamoto H, Suzuki S, Sugiyama N, et al. Tetrahydrobiopterin-responsive phenylalanine hydroxylase deficiency. J Pediatr 1999;135:375-8.
5. Keil S, Anjema K, van Spronsen FJ, Lambruschini N, Burlina A, Bélanger-Quintana A, et al. Long-term follow-up and outcome of phenylketonuria patients on sapropterin: a retrospective study. Pediatrics 2013;131:e1881-8.
6. Leuret O, Barth M, Kuster A, Eyer D, de Parscau L, Odent S, et al. Efficacy and safety of BH_4 before the age of 4 years in patients with mild phenylketonuria. J Inherit Metab Dis 2012;35:975-81.

50 Years Ago in *THE JOURNAL OF PEDIATRICS*

Familial Extrahepatic Biliary Atresia?

Krauss AN. J Pediatr 1964;65:933-7

In 1964, Krauss reported cholestasis in a pair of siblings. His diagnosis of "extrahepatic familial biliary atresia" can be referenced to highlight the growing understanding of the spectrum of neonatal cholestasis that has occurred over the past 50 years.

The "differential" diagnosis for neonatal cholestasis in the 1960s was fairly simple, consisting of 3 main categories: (1) biliary atresia, which constituted roughly 25% of cases; (2) viral induced injury—toxoplasmosis, other, rubella, cytomegalovirus, and herpes simplex virus (TORCH)—infections, which were identified in less than 10%; and (3) "neonatal hepatitis," a misleading term referring to infants whose histologic findings included giant cell transformation of unknown etiology that served as a wastebasket diagnosis for roughly 65% of the infants who presented with elevated liver enzymes and jaundice. "Neonatal hepatitis" was idiopathic and often classified as sporadic or familial depending on the history.

Today, the landscape of neonatal cholestasis is much more defined. Alpha-1 antitrypsin deficiency, metabolic diseases, progressive familial intrahepatic cholestasis, bile acid synthetic defects, and Alagille syndrome are only a few of the now well-described processes that have reduced the percentage of infants with idiopathic neonatal cholestasis to about 10% of cases. This exponential expansion of knowledge that has culminated in the current understanding of the biologic basis of neonatal cholestatic syndromes paralleled the growth and development of the new subspecialty of pediatric hepatology.[1]

Although the precise etiology of biliary atresia remains unknown, it has not been documented to reoccur in a family member subsequently. Therefore, re-visiting Krauss' report today, one cannot help but consider an alternative diagnosis. A leading candidate would be Alagille syndrome given the cardiac and renal abnormalities identified in the publication. Unfortunately for the brothers in Krauss' report, Daniel Allagille's seminal article describing the autosomal dominant, multisystem disorder that now carries his name would not be published for another 5 years.[2]

Despite the advances, looking forward to the next 50 years it is clear that there is work to be done. As noted, up to 10% of infants presenting today with jaundice and elevated liver biochemistries will be diagnosed with "idiopathic neonatal hepatitis." Understanding that the best therapeutic interventions are those that target key mechanisms of injury, it is paramount to continue to investigate the biological, molecular, genetic, and cellular contributions to this devastating disease to enable better treatment strategies that will change the outcome for affected children.

James E. Squires, MD, MS
Division of Gastroenterology
Advanced Hepatology
Cincinnati Children's Hospital Medical Center
Cincinnati, Ohio
http://dx.doi.org/10.1016/j.jpeds.2014.06.006

References

1. Balistreri WF. Growth and development of a new subspecialty: pediatric hepatology. Hepatology 2013;58:458-76.
2. Alagille D, Thomassin HE. L'atresie des voies biliares intrahepatiques avec voies biliaires extrahepatiques permeables chez l'enfant. Ann Med Interne (Paris) 1972;123:871-3.

Libertas Academica
FREEDOM TO RESEARCH

Open Access: Full open access to this and thousands of other papers at http://www.la-press.com.

Japanese Clinical Medicine

Dynamic Change in Cells Expressing IL-1β in Rat Hippocampus after Status Epilepticus

Satoru Sakuma[1], Daisuke Tokuhara[1], Hiroshi Otsubo[2], Tsunekazu Yamano[1] and Haruo Shintaku[1]

[1]Department of Pediatrics, Osaka City University Graduate School of Medicine, Osaka, Japan. [2]Division of Neurology, The Hospital for Sick Children, Toronto, Canada.

ABSTRACT

BACKGROUND: The time course of cytokine dynamics after seizure remains controversial. Here we evaluated the changes in the levels and sites of interleukin (IL)-1β expression over time in the hippocampus after seizure.

METHODS: Status epilepticus (SE) was induced in adult Wistar rats by means of intraperitoneal injection of kainic acid (KA). Subsequently, the time courses of cellular localization and IL-1β concentration in the hippocampus were evaluated by means of immunohistochemical and quantitative assays.

RESULTS: On day 1 after SE, CA3 pyramidal cells showed degeneration and increased IL-1β expression. In the chronic phase (>7 days after SE), glial fibrillary acidic protein (GFAP)—positive reactive astrocytes—appeared in CA1 and became IL-1β immunoreactive. Their IL-1β immunoreactivity increased in proportion to the progressive hypertrophy of astrocytes that led to gliosis. Quantitative analysis showed that hippocampal IL-1β concentration progressively increased during the acute and chronic phases.

CONCLUSION: IL-1β affects the hippocampus after SE. In the acute phase, the main cells expressing IL-1β were CA3 pyramidal cells. In the chronic phase, the main cells expressing IL-1β were reactive astrocytes in CA1.

KEYWORDS: interleukin-1β, status epilepticus, hippocampus, gliosis, reactive astrocyte

CITATION: Sakuma et al. Dynamic Change in Cells Expressing IL-1β in Rat Hippocampus after Status Epilepticus. *Japanese Clinical Medicine* 2014:5 25–32 doi:10.4137/JCM.S13738.

RECEIVED: November 27, 2013. **RESUBMITTED:** January 22, 2014. **ACCEPTED FOR PUBLICATION:** February 24, 2014.

ACADEMIC EDITOR: Yoshiyuki Hamamoto, Deputy Editor in Chief

TYPE: Original Research

FUNDING: This work was supported in part by a research grant for nervous and mental disorders from the Ministry of Health, Labour and Welfare of Japan, and a Houjinkai Fellowship Award from the Department of Pediatrics at Osaka City University Graduate School of Medicine.

COMPETING INTERESTS: Authors disclose no potential conflicts of interest.

CORRESPONDENCE: ssakuma@msic.med.osaka-cu.ac.jp

This paper was subject to independent, expert peer review by a minimum of two blind peer reviewers. All editorial decisions were made by the independent academic editor. All authors have provided signed confirmation of their compliance with ethical and legal obligations including (but not limited to) use of any copyrighted material, compliance with ICMJE authorship and competing interests disclosure guidelines and, where applicable, compliance with legal and ethical guidelines on human and animal research participants.

Introduction

Hippocampal gliosis, which is caused by pyramidal cell death induced by prolonged febrile convulsions, is an epileptic focus in patients with temporal lobe epilepsy (TLE).[1,2] In experimental studies, rats with kainic acid (KA)-induced status epilepticus (SE) develop spontaneous and recurrent seizures as well as pathologic hippocampal changes similar to those associated with human TLE; they are therefore considered an appropriate animal model of TLE.[3–6] Human and animal studies have both shown that inflammatory molecules, including cytokines, are key contributors to the seizure-associated progression of hippocampal gliosis.[7–10] Interleukin (IL)-1β is a major pro-inflammatory cytokine synthesized by macrophages, glial cells, and neuronal cells during infection and inflammatory processes.[11–13] Rats with KA-induced SE receiving intranasal administration of IL-1β showed repeated and prolonged hyperthermia-induced seizures with a significantly reduced onset time.[14] Furthermore, intrahippocampal injection of IL-1β extends the duration of KA-induced SE.[15,16] In contrast, treatment with an exogenous IL-1 receptor antagonist or overexpression of its endogenous form markedly inhibits neuronal injury induced by bicuculline or cerebral ischemia.[17,18]

Pretreatment with an IL-1β receptor antagonist significantly reduces the onset of pilocarpine-induced SE and damage to the blood–brain barrier in rats.[19]

A previous immunohistochemical study has shown that in the acute phase after KA administration, IL-1β is expressed in the stratum oriens and stratum radiatum of both the CA1 and CA3 areas of the hippocampus.[16] Another study has found diffuse IL-1β immunoreactivity throughout the hippocampus one to two days after SE.[9,16] By contrast, IL-1β expression is present on microglial cells in the granule and molecular cell layers as well as the hilum of the dentate gyrus within 24 hours after SE.[9,16] In the chronic phase (>7 days) after SE, reactive astrocytes in CA3 begin to express IL-1β,[10,20] as do some microglia in the same region at four weeks. Another report has demonstrated that glia in CA3 expressed IL-1β at 7 days, but not at 60 days, after SE in two of six spontaneously epileptic rats.[9]

Although this evidence supports an important role of IL-1β in the pathogenesis of both human and animal TLE, the cells expressing IL-1β in the development of hippocampal sclerosis and neuronal excitability vary depending on the study, and therefore their identity remains unclear. To determine which cells are affected by IL-1β in the process of hippocampal glial formation after SE, we investigated IL-1β expression in the hippocampus, focusing on pyramidal and glial cells at various time points after SE.

Materials and Methods

Animals and treatments. The animal committee of Osaka City University School of Medicine approved this study, which was conducted in accordance with the Guidelines for Use and Care of Experimental Animals. Eight-week-old male Wistar rats (180–200 g) were provided food and water ad libitum under a standard 12:12-hour light:dark cycle. Rats were injected first with KA (10 mg/kg) intraperitoneally to induce SE, and then two hours after seizure onset with diazepam (10 mg/kg) to abort the SE.[5] Seizure severity was determined by using the Racine scale: stage 1, mouth and facial movements; stage 2, head nodding; stage 3, forelimb clonus; stage 4, rearing; and stage 5, rearing and falling.[21] Four control rats received saline. A total of 16 rats were anesthetized with sodium pentobarbital on days 1 (12–24 hours after SE), 7, 14, and 21 (n = 4 at each time point) after KA administration and then transcardially perfused with phosphate-buffered saline (PBS, pH 7.4). A total of three rats died owing to SE (one each on days 1, 7, and 14).

After sacrifice, the brains of the rats were quickly removed. The right hemisphere of each brain was post-fixed by immersion in 4% paraformaldehyde overnight at 4°C, then embedded in Tissue-Tek optimum cutting temperature (OCT) compound (Miles, Elkhart, IN, USA), frozen with liquid nitrogen, and sliced into coronal frozen sections (thickness, 20 μm) with a cryostat. The left hemisphere of each brain was immediately prepared for quantitative analysis of IL-1β as detailed below.

IL-1β immunohistochemistry. Several sections from each rat brain were examined for IL-1β localization by means of an immunohistochemical approach; other sections were assessed for the co-localization of IL-1β and glial fibrillary acidic protein (GFAP) by means of a double-label immunofluorescence technique. For the immunohistochemical study, a commercially available rabbit polyclonal anti-IL-1β antibody (diluted 1:500; sc-1251, Santa Cruz Biotechnology, Santa Cruz, CA, USA) was used. An anti-human monoclonal GFAP antibody (diluted 1:50; 03-61011, American Research Products, Belmont, MA, USA) was used in the assessment of GFAP localization. Double-label immunofluorescence staining of IL-1β (sc-1251 diluted 1:250) and GFAP (03-61011), as well as immunohistochemistry, was carried out as described previously.[5] To assess the specificity of the primary antibodies, additional sections were subjected to immunohistochemical processing without primary antibody and used as negative controls; these sections were also stained with hematoxylin and eosin.

Quantitative analysis of IL-1β. To assess protein levels, rats were anesthetized before SE and on days 1 (n = 3; 12–24 hours after SE), 7 (n = 3), 14 (n = 3), and 21 (n = 4) after SE. The left hemisphere of each brain was quickly removed, and the hippocampus was dissected on ice and individually homogenized in PBS containing a protease inhibitor cocktail. Homogenates were centrifuged at 4°C, and the supernatants were recovered as samples. IL-1β was measured by using a Bio-Plex Cytokine Assay kit (171-K11070, Bio-Rad Laboratories, Hercules, CA, USA) according to the manufacturer's instructions. Briefly, premixed standards were reconstituted by using the provided standard diluents, and a standard curve (0.975–8000 pg/mL) was constructed. An anti-cytokine bead stock solution was added to the wells of a 96-well filter plate. After the filters were washed, the standards and samples (50 μL/well) were added to the wells. Plates were incubated for 30 minutes at room temperature and then washed again, after which 25 μL of detection antibodies was added to each well. After the plates were again incubated and washed as described above, 50 μL of streptavidin–phycoerythrin was added to each well, and the plates were incubated for a further 10 minutes before being similarly washed. Finally, the beads were resuspended in Bio-Plex assay buffer. Plates were read on the Bio-Plex suspension array system (Bio-Rad), and the data were analyzed by using Bio-Plex Manager version 5.0. Statistical analysis was performed with the SSPS 16.0 software (SPSS, Chicago, IL, USA) by using one-way analysis of variance.

Results

Clinical features of seizures and histological findings. Within one hour after KA injection, all rats developed stage 5 seizures according to the Racine scale.[21] After the SE was aborted with diazepam, rats developed spontaneous generalized tonic–clonic seizures with a latency of five to seven days.

The histologic changes that occurred after the KA-induced SE were similar to those seen in our previous studies.[3–5] The numbers of pyramidal cells in the control rats were 1083 ± 44, 1183 ± 169, 1150 ± 150, and 983 ± 130 cells/mm^2 (mean ± SE) in the CA1, CA2, CA3, and CA4 regions of the hippocampus, respectively. The numbers of pyramidal cells on day 7 after SE were 867 ± 109, 808 ± 156, 483 ± 93, and 517 ± 60 cells/mm^2 in CA1, CA2, CA3, and CA4, respectively. The numbers of pyramidal cells on day 14 after SE were 683 ± 72, 517 ± 93, 500 ± 58, and 433 ± 33 cells/mm^2 in CA1, CA2, CA3, and CA4, respectively. The numbers of pyramidal cells on day 21 after SE were 133 ± 33, 500 ± 104, 333 ± 93, and 367 ± 44 cells/mm^2 in CA1, CA2, CA3, and CA4, respectively.[5] Hematoxylin and eosin staining revealed pyknotic pyramidal cells in CA1 on day 1 (Fig. 1B); the degree of pyramidal cell loss in CA1 gradually increased from day 7 to day 21 after SE (Fig. 1C). Pyramidal cell death also occurred in CA3 (rate of loss after SE, 71%) and CA4 (63%) but to a lesser extent than that in CA1 (89%) at day 21. GFAP-immunoreactive astrocytes with subsequent hypertrophy increased from day 7 to day 21 in proportion to pyramidal cell loss, which resulted in hippocampal gliosis (Figs. 1D–H).

IL-1β immunoreactivity in rat hippocampus during the acute phase after SE. IL-1β was weakly expressed in the cytoplasm of CA1 and CA3 pyramidal cells in the control rat hippocampus (Figs. 2D, G, I, M). However, in rats with SE, IL-1β expression increased transiently in the cytoplasm of the remaining pyramidal cells in the CA3 region beginning at day 1 after SE (Figs. 2H, N). Cytoplasmic IL-1β expression in pyramidal cells in CA3 was greater than that in CA1 on day 1 after SE (Figs. 2E, H, K, N; Table 1).

IL-1β immunoreactivity in rat hippocampus during the chronic phase (>7 days) after SE. At day 7 after SE onset, pyramidal cells in CA1 lacked IL-1β immunoreactivity. However, those in CA3 were still positive for IL-1β. In contrast, reactive astrocyte-like cells emerging in CA1

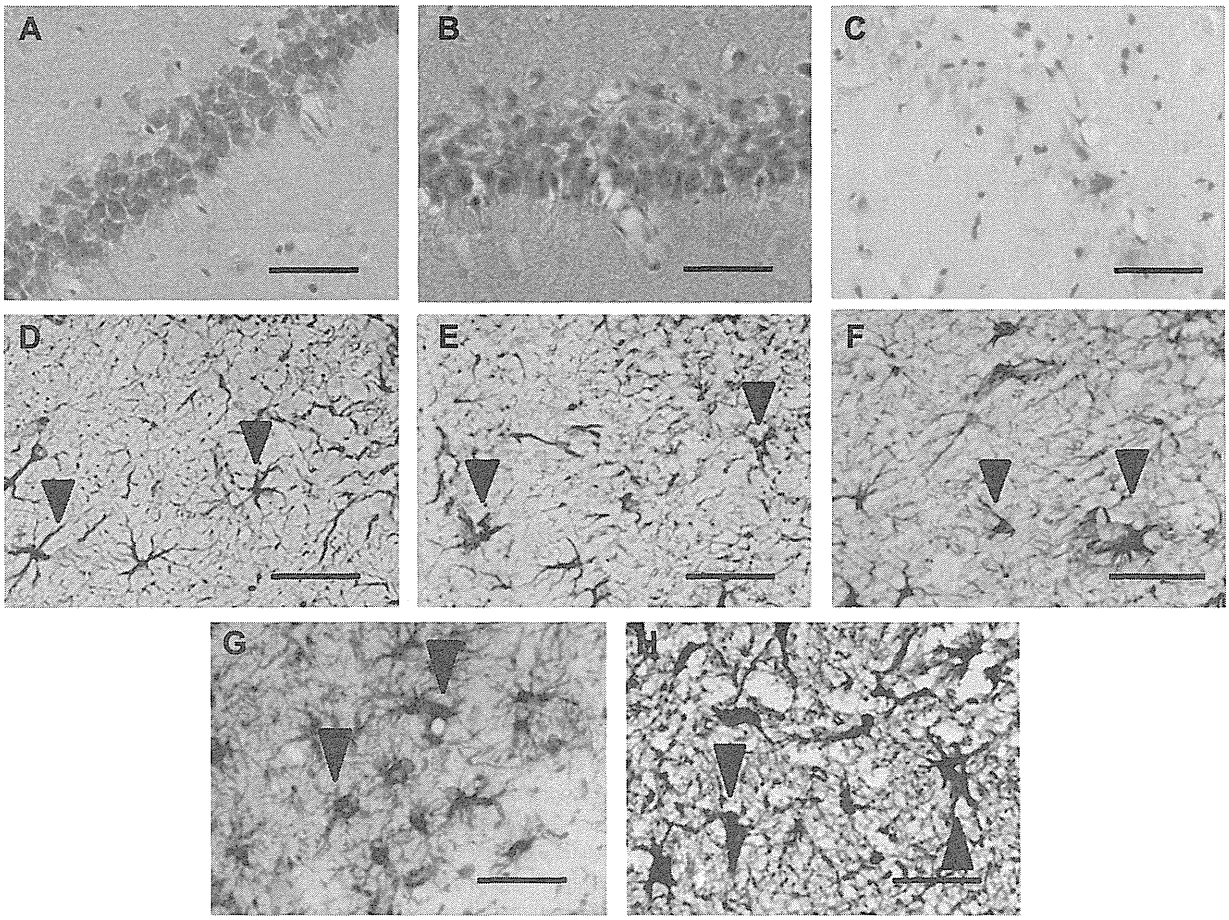

Figure 1. Hematoxylin and eosin staining and GFAP staining in the rat hippocampus. (**A–C**) Hematoxylin and eosin staining in the CA1 region of control rats without SE and KA-treated rats after SE. (**A**) CA1 region at control rat hippocampus. Pyramidal cells were not degenerated. (**B**) CA1 region on day 1 after SE. Pyknotic pyramidal cells were seen in the CA1 region of rat hippocampus. (**C**) CA1 region on day 21 after SE. Most pyramidal cells were lost. (**D–H**) GFAP staining in the CA1 region of control rats without SE and KA-treated rats after SE. (**D**) CA1 region at control rat hippocampus. A few GFAP positive cells were observed. (**E**) CA1 region on day 1 after SE. GFAP positive cells on day 1 after SE have no change compared to control rats (**D**). (**F**) CA1 region on day 7 after SE. Increased numbers of astroglia-like cells were observed. (**G**) CA1 region on day 14 after SE. The number of astroglia-like cells in (**H**) CA1 region on day 21 after SE. GFAP-immunoreactive astroglia-like cells were increased in proportion to the progressive hypertrophy of astrocytes, forming gliosis (**G**, **H**).

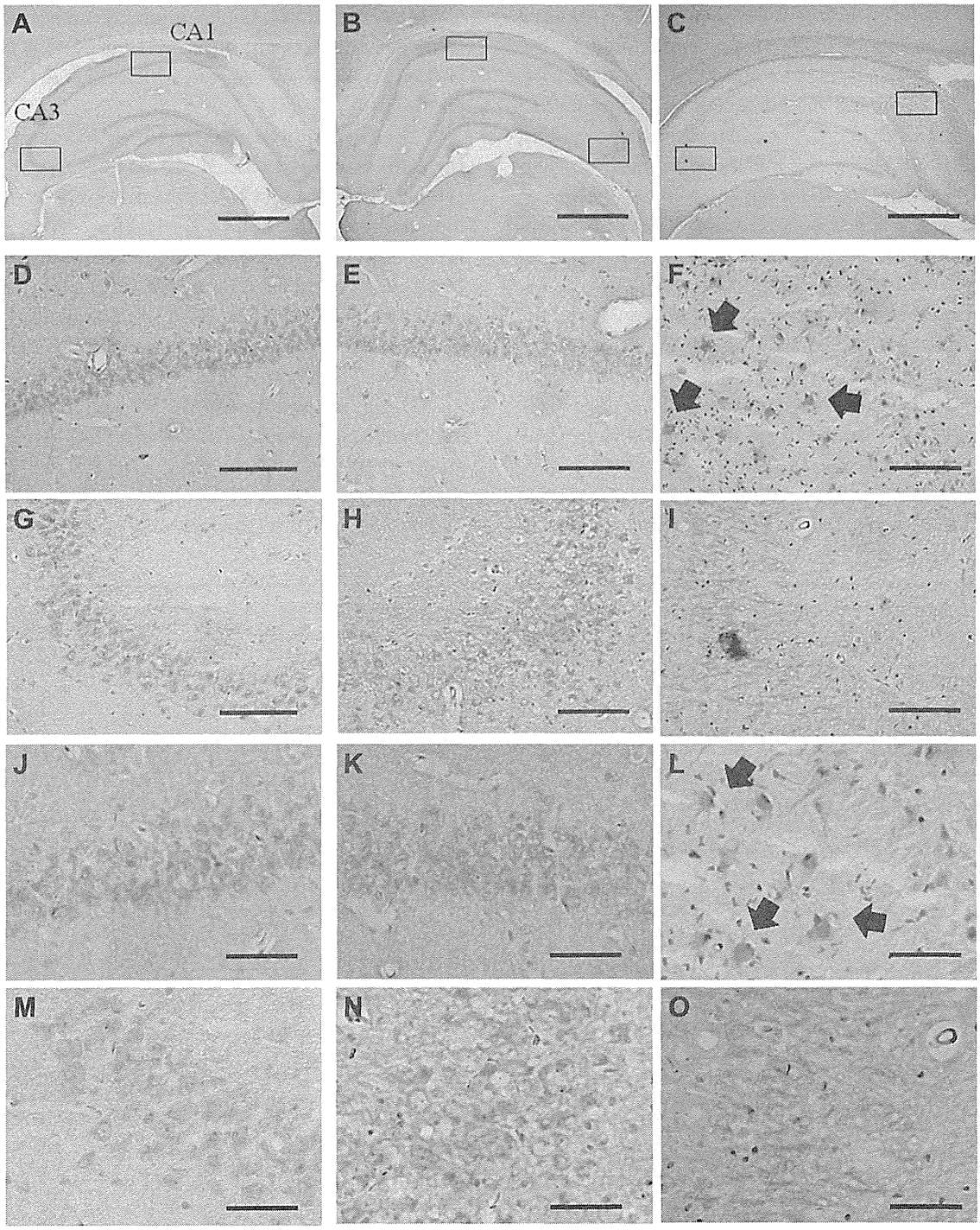

Figure 2. IL-1β immunoreactivity in the hippocampus of control rat without SE and after SE. (**A**, **D**, **G**, **J**, **M**) Expression of IL-1β at control rat hippocampus. (**A**) Expression of IL-1β at the hippocampus of control rat without SE in low-power magnification. Scale bar = 1 mm. (**D**) CA1 region of control rat in intermediate power magnification. (**G**) CA3 region of control rat in intermediate power magnification. **D**, **G**; scale bar = 100 μm. (**J**) CA1 region of control rat in high-power magnification. (**M**) CA3 region of control rat in high-power magnification. **J**, **M**; scale bar = 50 μm. Expression of IL-1β was faintly observed in the pyramidal cells at CA1 (**D**, **J**) and CA3 (**G**, **M**) regions. (**B**, **E**, **H**, **K**, **N**) Expression of IL-1β at day 1 after SE. (**B**) Expression of IL-1β at the hippocampus at day 1 after SE in low power magnification. Scale bar = 1 mm. (**E**) CA1 region at day 1 after SE in intermediate power magnification. (**H**) CA3 region at day 1 after SE in intermediate power magnification. **E**, **H**; scale bar = 100 μm. (**K**) CA1 region at day 1 in high power magnification. (**N**) CA3 region at day 1 after SE in high power magnification. IL-1β expression increased transiently in the cytoplasm of the remaining pyramidal cells in the CA3 region beginning on day 1 after SE (**H**, **N**). Expression of IL-1β in the cytoplasm of pyramidal cells at CA3 was greater than that at CA1 on day 1 after SE (**E**, **H**, **K**, **N**; Table 1). **K**, **N**; scale bar = 50 μm. (**C**, **F**, **I**, **L**, **O**) Expression of IL-1β at day 21 after SE. (**B**) Expression of IL-1β at the hippocampus at day 21 after SE in low-power magnification. Scale bar = 1 mm. (**E**) CA1 region at day 21 after SE in intermediate power magnification. (**H**) CA3 region at day 21 after SE in intermediate power magnification. **F**, **I**; scale bar = 100 μm. (**F**) CA1 region at day 21 in high power magnification. (**N**) CA3 region at day 21 after SE in high power magnification. Reactive astrocyte-like cells emerging in CA1 showed IL-1β immunoreactivity on day 7. This immunointensity increased in proportion to progressive hypertrophy until day 21. **L**, **O**; scale bar = 50 μm.

Table 1. Expression of IL-1β in the rat hippocampus.

HIPPOCAMPAL REGION	CONTROL	1 DAY AFTER SE	7 DAY AFTER SE	14 DAY AFTER SE	21 DAY AFTER SE
Pyramidal cells					
CA1	+	+	+	–	–
CA3	+	++	+	–	–
Reactive astrocytes					
CA1	–	–	+	++	+++
CA3	–	–	+	++	++

Notes: Degree of IL-1β-immunoreactive cells: –, no staining; +, faint; ++, frequent; +++, predominant.

showed IL-1β immunoreactivity at day 7 after SE. Immunointensity increased in proportion to progressive hypertrophy until day 21 when the pyramidal cells, which had degenerated because of cell death, lacked IL-1β expression (Figs. 2F, I, L, O; Table 1).

To confirm that the observed IL-1β–immunoreactive astrocyte-like cells were actually reactive astrocytes, we performed double-label immunofluorescence for IL-1β (Fig. 3A) and GFAP (Fig. 3B). Co-localization of IL-1β and GFAP immunoreactivities was confirmed in these reactive astrocytes, which first appeared in CA1 at day 7 and had become numerous at day 21 after SE (Fig. 3C).

Quantitative analysis of IL-1β. Quantitative analysis of IL-1β in control rats without SE (n = 4) and of KA-treated rats on days 1 (n = 3), 7 (n = 3), 14 (n = 3), and 21 (n = 4) after SE onset showed hippocampal IL-1β concentrations of 144 ± 51 pg/mL, 570 ± 180 pg/mL, 2770 ± 798 pg/mL, 1732 ± 344 pg/mL, and 1806 ± 174 pg/mL (mean ± SE), respectively (Fig. 4). At day 1 after SE onset, IL-1β concentration was approximately four times higher in KA-treated rats than in control rats without SE; however, no significant difference in IL-1β concentration in the hippocampus was found between KA-treated rats on day 1 after SE and control rats without SE (P = 0.770). In contrast, in the chronic phase on days 7, 14, and 21 after SE onset, IL-1β concentrations were approximately 20, 12, and 12 times higher, respectively, in KA-treated rats than in control rats without SE. Statistically, the hippocampal IL-1β concentration in KA-treated rats was significantly higher on day 7 (P = 0.003), day 14 (P = 0.029), and day 21 (P = 0.017) than that in control rats without SE.

Discussion

IL-1β is a key pro-inflammatory cytokine in the formation of hippocampal sclerosis after SE; therefore, understanding which cells express IL-1β and the dynamics of IL-1β expression in the hippocampus after SE is important for establishing future therapeutic strategies. Here we elucidated the detailed dynamics of IL-1β expression in the hippocampus. A previous study found that in control rats there is only slight expression of IL-1β in the CA3 region of the hippocampus;[16] however, a different study demonstrated prominent IL-1β expression in scattered neurons of the dentate gyrus and less expression in the neurons in CA3 and CA1.[9] Other studies have failed to detect any IL-1β immunoreactivity at all.[20,22] In the present study, IL-1β was weakly expressed in pyramidal neurons in CA3, showing that IL-1β is not highly expressed in the hippocampus under normal circumstances in non-epileptic animals. Furthermore, our immunohistochemical and quantitative investigations clearly demonstrated that IL-1β is involved in hippocampal degeneration after SE and that there are differences in IL-1β expression between the acute and chronic phases.

A previous study has shown that three hours after KA administration, IL-1β is expressed on the stratum oriens and

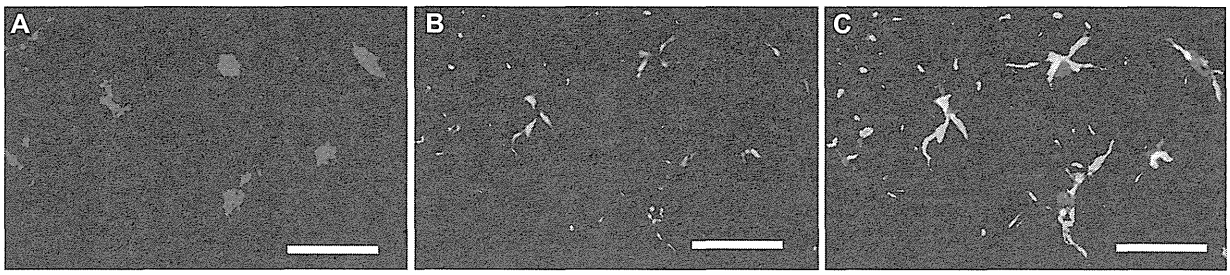

Figure 3. Double-label immunofluorescence staining of IL-1β and GFAP. Co-localization of IL-1β (red, **A**) and GFAP (green, **B**) is shown with an immunofluorescence method. Co-localization is visualized in yellow in the merged image (**C**). Double-label fluorescent immunohistochemistry clarified that reactive astrocytes expressed IL-1β. Scale bar = 50 μm.

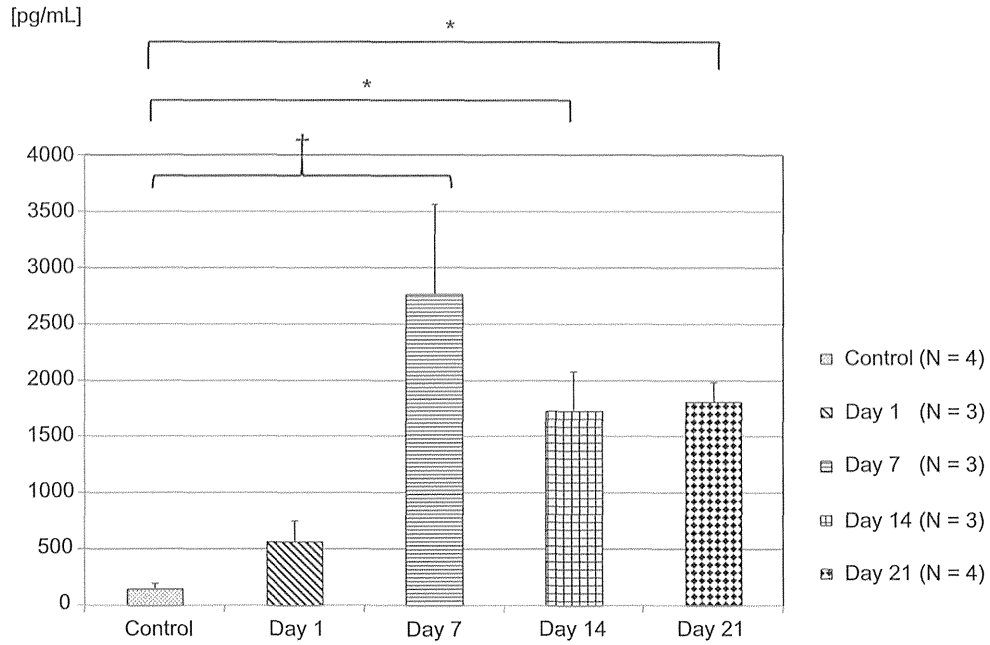

Figure 4. Total IL-1β expression in the hippocampus after SE. The total expression level IL-1β in the hippocampus measured by using Luminex technology was significantly elevated from day 1 after SE and maintained till day 21 ($P < 0.01$). Asterisks (*) and daggers (†) indicate significant differences ($P < 0.05$ and $P < 0.005$, respectively) from the value for the control group.

stratum radiatum in CA1, and the stratum oriens, stratum radiatum, and stratum lucidum in CA3.[15] Other reports have stated that IL-1β immunoreactivity is present throughout the hippocampus 24 hours after KA administration and 48 hours after SE onset.[9,16] IL-1β is also expressed on microglial cells in the granule and molecular cell layers and hilus of the dentate gyrus within 24 hours after seizures begin.[9,16] In the present study, IL-1β was expressed on pyramidal neurons in the CA3 region at one and three days after SE. Although the cellular location of IL-1β in our study during the acute phase was not completely consistent with previous studies, IL-1β expression is likely similarly expressed in the pyramidal neurons during the acute phase after SE.

At 60 days after SE, IL-1β is expressed in CA3 by pyramidal neurons and interneurons close to the inner border of the granule cells of the dentate gyrus.[23] Reactive astrocytes prominently express IL-1β,[10,20] and some microglia in CA3 express IL-1β at four weeks after SE onset.[10] Another report has demonstrated IL-1β immunoreactivity in the CA3 glia at 7 days, but not 60 days, after SE.[9] In the present study, we noted IL-1β expression on reactive astrocytes similar to that shown by previous studies. Although our current findings basically support the expression pattern of pro-inflammatory cytokines that has been previously elucidated, they make several additional contributions. Specifically, immunohistologic methods revealed changes in the localization of IL-1β immunoreactivity across time as it moved from pyramidal cells to reactive astrocytes. In addition, we qualitatively analyzed IL-1β levels in the acute through chronic phase after SE onset. By combining the results of previous studies with the present results, the conclusion that reactive astrocytes are important as the main cells expressing IL-1β during the chronic phase after SE is further strengthened. Because reactive astrocytes are components of hippocampal gliosis, IL-1β can be considered a key factor in glial formation.

Another important finding is that the localization of IL-1β immunoreactivity changes over time and moves from pyramidal cells to reactive astrocytes. Our previous study showed that the survival rate of pyramidal cells in CA1 was 77% at day 7 after SE but only 12% at day 21, and that the survival of these cells in CA3 was 43% at day 7 compared with 29% at day 21.[5] Regardless of the decrease in pyramidal cell number, our present microbead-based assay demonstrated that the total level of IL-1β expression in the hippocampus increased significantly between days 7 and 21 after SE. Simultaneously, the rats developed spontaneous seizures, and reactive astrocytes appeared in the hippocampus at day 7. These findings indicate a transition in the production of IL-1β from pyramidal cells during the acute phase to reactive astrocytes during the chronic phase after SE onset.

Regarding the role of reactive astrocytes, various reports have addressed the pathomechanism underlying the role of reactive astrocytes in epileptogenesis. Glutamine synthetase, which converts glutamate released at excitatory synapses to glutamine, is predominantly expressed in astrocytes.[24–26] Loss of glutamine synthetase is particularly pronounced in areas of the human mesial TLE hippocampus with astroglial proliferation.[24] In addition, several recent studies have reported that adenosine kinase (ADK) in reactive astrocytes affects seizure development. Upregulation of ADK in astrocytes

has been noted in cases of experimental and human TLE.[27] IL-1β and lipopolysaccharide both increase the expression of ADK in cultured human astrocytes, as assessed by western blot analysis. In mice, ADK is a marker for epileptogenesis.[28] Furthermore, adenosine acts as an anticonvulsant that has a neuroprotective role via the adenosine A1 receptor.[29] Another study reported that a complex mixture of signal molecules is released into the extracellular milieu of high-mobility group box 1 (HMGB1)-stimulated astrocytes and that this mixture is functionally involved in the stimulation of monocyte chemotaxis.[30] Human astrocyte cultures obtained during surgery for malformation of cortical development have shown that nuclear to cytoplasmic translocation of HMGB1 is induced by IL-1β.[31] In our present study, IL-1β was expressed on reactive astrocytes, and not pyramidal cells, of the hippocampus during the chronic phase after SE, suggesting an IL-1β-associated role of reactive astrocytes in epileptogenesis during this stage.

In regard to the neuroexcitatory mechanism of IL-1β, *N*-methyl-D-aspartate receptor function is enhanced by IL-1β through the activation of tyrosine kinases and subsequent phosphorylation of the NR2A/B subunit.[32] This implies that IL-1β contributes to glutamate-mediated neurodegeneration. Other research has indicated that IL-1β affects astrocytes by inhibiting the astrocytic reuptake of glutamate.[33] In addition, IL-1β can increase neuronal glutamate release via the activation of inducible nitric oxide synthase in astrocytes.[34] Together, these studies indicate that inflammatory cytokines chronically influence epileptogenesis. Examination of the time course of the expression and distribution of inflammatory cytokines after SE onset is crucial, and in this regard, our current findings support the results of previous studies.

TLE with hippocampal gliosis is often refractory to treatment. Recent clinical studies have demonstrated increased expression of pro-inflammatory molecules in the neurons and glia of brain tissue obtained from patients treated surgically for drug-resistant epilepsy.[35,36] Excessive levels of pro-inflammatory cytokines destroy neurons and may lead to seizures. In the context of recurrent seizures, our results suggest that the repeated seizures promoted by IL-1β may expand the epileptic focus and render seizures intractable to therapy.

In conclusion, our study characterized the time course of IL-1β expression in the hippocampus after SE in the acute and chronic phases by using immunohistochemical and quantitative methods. Our results indicated that IL-1β affects the rat hippocampus after SE, especially during the chronic phase. In the acute phase, the main cells expressing IL-1β were pyramidal cells in CA3, whereas in the chronic phase, the main cells expressing IL-1β were reactive astrocytes in CA1.

Author Contributions

Conceived and designed the experiments: SS, TY. Analyzed the data: SS. Wrote the first draft of the manuscript: SS. Contributed to the writing of the manuscript: DT, TY. Agree with manuscript results and conclusions: SS, DT, HO, TY, HS. Jointly developed the structure and arguments for the paper: DT, HO, TY, HS. Made critical revisions and approved final version: SS, DT, HS. All authors reviewed and approved of the final manuscript.

REFERENCES

1. Hamati-Haddad A, Abou-Khalil B. Epilepsy diagnosis and localization in patients with antecedent childhood febrile convulsions. *Neurology*. 1998;50(4): 917–922.
2. Lawson JA, Vogrin S, Bleasel AF, et al. Predictors of hippocampal, cerebral, and cerebellar volume reduction in childhood epilepsy. *Epilepsia*. 2000;41(12): 1540–1545.
3. Tokuhara D, Yokoi T, Nakajima R, Hattori H, Matsuoka O, Yamano T. Time course changes of estrogen receptor alpha expression in the adult rat hippocampus after kainic acid-induced status epilepticus. *Acta Neuropathol*. 2005;110(4): 411–416.
4. Tokuhara D, Sakuma S, Hattori H, Matsuoka O, Yamano T. Kainic acid dose affects delayed cell death mechanism after status epilepticus. *Brain Dev*. 2007; 29(1):2–8.
5. Sakuma S, Tokuhara D, Hattori H, Matsuoka O, Yamano T. Expression of estrogen receptor alpha and beta in reactive astrocytes at the male rat hippocampus after status epilepticus. *Neuropathology*. 2009;29(1):55–62.
6. Pernot F, Heinrich C, Barbier L, et al. Inflammatory changes during epileptogenesis and spontaneous seizures in a mouse model of mesiotemporal lobe epilepsy. *Epilepsia*. 2011;52(12):2315–2325.
7. Griffin WS, Yeralan O, Sheng JG, et al. Overexpression of the neurotrophic cytokine S100 beta in human temporal lobe epilepsy. *J Neurochem*. 1995;65(1): 228–233.
8. Crespel A, Coubes P, Rousset MC, et al. Inflammatory reactions in human medial temporal lobe epilepsy with hippocampal sclerosis. *Brain Res*. 2002; 952(2): 159–169.
9. De Simoni MG, Perego C, Ravizza T, et al. Inflammatory cytokines and related genes are induced in the rat hippocampus by limbic status epilepticus. *Eur J Neurosci*. 2000;12(7):2623–2633.
10. Kim JE, Choi HC, Song HK, et al. Levetiracetam inhibits interleukin-1 beta inflammatory responses in the hippocampus and piriform cortex of epileptic rats. *Neurosci Lett*. 2010;471(2):94–99.
11. Hopkins SJ, Rothwell NJ. Cytokines and the nervous system. I: expression and recognition. *Trends Neurosci*. 1995;18(2):83–88.
12. Le Feuvre RA, Brough D, Iwakura Y, Takeda K, Rothwell NJ. Priming of macrophages with lipopolysaccharide potentiates P2X7-mediated cell death via a caspase-1-dependent mechanism, independently of cytokine production. *J Biol Chem*. 2002;277(5):3210–3218.
13. Lee SH, Kim BJ, Kim YB, et al. IL-1beta induction and IL-6 suppression are associated with aggravated neuronal damage in a lipopolysaccharide-pretreated kainic acid-induced rat pup seizure model. *Neuroimmunomodulation*. 2012;19(5): 319–325.
14. Fukuda M, Hino H, Suzuki Y, Takahashi H, Morimoto T, Ishii E. Postnatal interleukin-1beta enhances adulthood seizure susceptibility and neuronal cell death after prolonged experimental febrile seizures in infantile rats. *Acta Neurol Belg*. 2013 Sep 4. [Epub ahead of print].
15. Vezzani A, Moneta D, Richichi C, et al. Functional role of inflammatory cytokines and antiinflammatory molecules in seizures and epileptogenesis. *Epilepsia*. 2002;43(suppl 5):30–35.
16. Vezzani A, Conti M, De Luigi A, et al. Interleukin-1beta immunoreactivity and microglia are enhanced in the rat hippocampus by focal kainate application: functional evidence for enhancement of electrographic seizures. *J Neurosci*. 1999;19(12):5054–5065.
17. Vezzani A, Moneta D, Conti M, et al. Powerful anticonvulsant action of IL-1 receptor antagonist on intracerebral injection and astrocytic overexpression in mice. *Proc Natl Acad Sci U S A*. 2000;97(21):11534–11539.
18. Rothwell N. Interleukin-1 and neuronal injury: mechanisms, modification, and therapeutic potential. *Brain Behav Immun*. 2003;17(3):152–157.
19. Marchi N, Fan Q, Ghosh C, et al. Antagonism of peripheral inflammation reduces the severity of status epilepticus. *Neurobiol Dis*. 2009;33(2): 171–181.
20. Maroso M, Balosso S, Ravizza T, et al. Interleukin-1beta biosynthesis inhibition reduces acute seizures and drug resistant chronic epileptic activity in mice. *Neurotherapeutics*. 2011;8(2):304–315.
21. Racine RJ. Modification of seizure activity by electrical stimulation. II. Motor seizure. *Electroencephalogr Clin Neurophysiol*. 1972;32(3):281–294.